This document contains a post-print version of the paper

# Application of an Off-Gas Analysing System to Control Oxidation during Stainless Steelmaking in an EAF

authored by V. Y. Risonarta, T. Echterhof, H. P. Jung, C. Beiler, S. Lenz, M. Kirschen, H. Pfeifer

and published in *steel research international*

Link to the original paper:

http://dx.doi.org/10.1002/srin.201000134

Read more papers from the Department for Industrial Furnaces and Heat Engineering or get this document at:

https://www.iob.rwth-aachen.de/en/research/publications/

Contact

Department for Industrial Furnaces and Heat Engineering
RWTH Aachen University
Kopernikusstr. 10
52074 Aachen, Germany

Website: www.iob.rwth-aachen.de/en/
E-mail: contact@iob.rwth-aachen.de
Phone:  +49 241 80 25936
Fax:     +49 241 80 22289

# APPLICATION OF THE OFF-GAS ANALYSING SYSTEM TO CONTROL ELEMENTS OXIDATION DURING STAINLESS STEELMAKING IN AN EAF

V. Y. Risonarta[1], T. Echterhof[1], H. P. Jung[2], C. Beiler[2], S. Lenz[2], M. Kirschen[1,3], H. Pfeifer[1]

[1]Department for Industrial Furnaces and Heat Engineering, RWTH Aachen University
Kopernikusstraße 16, D-52074 Aachen, Germany

[2]Deutsche Edelstahlwerke GmbH
Obere Kaiserstraße, D-57078 Siegen, Germany

[3]present address: RHI AG
Magnesitstraße 2, A-8700 Leoben, Austria

*Synopsis: During stainless steelmaking in the electric arc furnace at Deutsche Edelstahlwerke GmbH, oxygen is injected to oxidize unwanted tramp elements mainly carbon and silicon. Unfortunately the injected oxygen also oxidizes valuable elements, e.g. chromium and iron, which causes an economical loss and a negative environmental effect. Since the temperature and dilution techniques to minimise chromium oxidation are seldom applied in the electric arc furnace, a new strategy to minimise chromium oxidation has to be developed. By using a continuous off-gas analysing system, this paper proposes a new strategy to minimise chromium oxidation by monitoring the oxidation products in the off-gas, i.e. CO and $CO_2$. During stainless steelmaking in the electric arc furnace, for which initial carbon and silicon input cannot be precisely known due to imprecise scrap analysis, the installed off-gas analysing system should provide precise information concerning an efficient oxygen injection. This then directly prevents excess chromium and iron oxidation. A continuous off-gas analysing system installed at Deutsche Edelstahlwerke GmbH delivers a promising result for future applications. During the plant trial, the efficiency of oxygen injection as well as the chromium and iron yields were increased.*

**Key Words: chromium scorification, stainless steel, off-gas analysing system, electric arc furnace**

## Introduction

Oxygen is injected during stainless steelmaking in the electric arc furnace, EAF, to oxidize unwanted tramp elements, mainly carbon and silicon, to the target level for tapping. Unfortunately, silicon and carbon oxidation by a high volume flow rate of oxygen injection is accompanied by an extensive chromium oxidation from liquid steel to slag. This is due to the less noble property of chromium, i.e. higher affinity to oxygen and oxidation at lower oxygen activities. Approximately 97 % of all chromium loss during EAF-based stainless steelmaking takes place in the EAF [1]. Meanwhile, chromium-alloy price had dramatically increased for the past several years. Stainless steel producers therefore have to minimise chromium loss during stainless steelmaking in the EAF due to its high price.

Apart from the economical reason, chromium oxidation during stainless steelmaking should be minimized since the formation of Cr species in leachates of EAF slag deposits and dusts has a negative environmental effect, which leads for special measures and causes an additional cost during the EAF process.

Known metallurgical strategies to decrease chromium oxidation during oxygen injection into liquid steel, i.e. operation at very high temperature of liquid steel, decrease of the CO activity by dilution of the injected argon gas or by vacuum technology, are not applied in the EAF. A new strategy to increase the efficiency of oxygen injection, which then directly decreases the chromium and iron loss to slag, has therefore to be developed. This new strategy is performed by controlling the oxidation process during the refining period. Many research efforts had been dedicated to developing a good control system of elements oxidation during the refining process through an in-situ slag analysis, e.g. [2-3]. Unlike the approach used in those researches, another approach is used in this research by monitoring the oxidation products in off-gas, i.e. CO and $CO_2$. The off-gas analysing system will provide precise information to control the efficiency of oxygen injection and the critical points of silicon and carbon oxidation. The latter defines the end of the efficient oxygen injection which directly prevents excess chromium and iron oxidation.

**Thermodynamic Simulation**

The input data used in this simulation is an exemplary industrial heat at Deutsche Edelstahlwerke GmbH (DEW). The compositions of scraps, alloys, and slag additives before the start of the refining period are sorted according to their chemical composition (**Table 1**). The Factsage thermodynamic databases [4] are then used to generate a free energy data file for the used set of elements and their corresponding phases. The amount of oxygen injection was given in a step amount and increas-

ing for each 100 kg $O_2$. After the equilibrium steel and slag compositions as well as each corresponding mass are determined from the thermodynamic simulation, the mass of oxidized elements are presented as sum of each oxide forms (**Figure 1**).

**Table 1.** Data input for thermodynamic simulation

| Elements input | Iron, carbon, silicon, manganese, chromium, nickel, molybdenum, copper, aluminium, CaO, MgO, CaO, MgO, $SiO_2$, $Al_2O_3$. |
|---|---|
| Temperature | 1500 to 1700 °C |
| Oxygen injection | 0 to 25 kg/t |
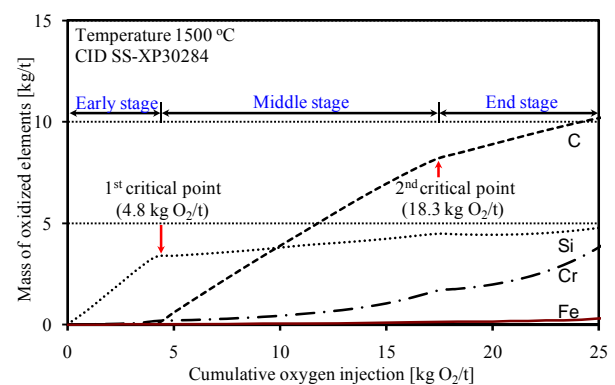


**Figure 1.** Result of thermodynamic simulation of elements oxidation (for an exemplary industrial heat)

Since the result of thermodynamic simulation is correlated with the measurement data of the off-gas analysing system, discussion concerning the result of thermodynamic simulation in this paper is emphasized on the decarburization process. For this reason, two critical points regarding the decarburization process can be identified in the simulation result. The first critical point is correlated with the start of the intensive decarburization, which takes place directly after the end of the intensive silicon oxidation. Meanwhile the second critical point is correlated with the decreasing gradient of decarburization. The result of thermodynamic simulation shows the existence of three stages of oxygen injection with regards to the decarburization process, i.e. the early stage, the middle stage, and the end stage. The first critical point ends the early stage. The middle stage is between the first and the second criti-

cal points while the end stage starts after the second critical point appears.

The injected oxygen favours to intensively oxidize silicon in the early stage before the first critical point appears, i.e. at 4.8 kg $O_2$/t for this particular heat. In the middle stage, oxygen starts to intensively oxidize chromium and carbon. In this stage, the cumulative oxidized carbon increases linearly with an increasing cumulative oxygen injection while chromium oxidation follows an exponential path. After the carbon concentration reaches its critical value, $[C]_{critical}$, the second critical point appears, i.e. at 18.3 kg $O_2$/t for this particular heat. Carbon oxidation starts to decrease in the end stage. This can be seen through a lower gradient of cumulative oxidized carbon with an increasing cumulative oxygen injection. On the other hand, the intensive chromium oxidation continues in the end stage. The intensive iron oxidation starts in the end stage. This simulation result also shows that chromium oxidation is thermodynamically more favourable than iron oxidation which can be seen from the intensive chromium oxidation since the middle stage.

**Industrial Investigation on the Oxidation Process**
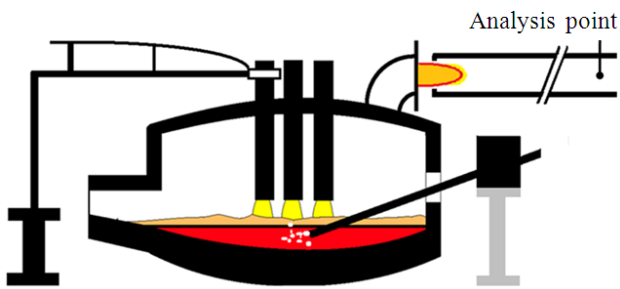


**Figure 2.** The analysis point at the EAF's primary dedusting system

Following the result of the thermodynamic simulation, an off-gas analysing system to investigate the oxidation process during the refining period was installed at the EAF's primary dedusting system. The industrial investigation performed by RWTH Aachen University used the off-gas analysing system from Emerson. Measurement of off-gas composition was performed at the hot gas duct near the EAF elbow, e.g. [5], and after post-combustion. The off-gas analysis near the EAF elbow minimises the influence of infiltrating air at the gap between the EAF's elbow and the off-gas dedusting system. However, Kirschen [6] demonstrated inhomogen distributions in radial direction of composition, temperature, and volume flow of the off-gas. The installation of the off-gas sampling lances in a particular distance to the EAF elbow resulted in longer service time of the off-gas measurement lances. Meanwhile, the infiltration of air into the off-gas does not influence the determination of the critical points of decarburization. For these reasons, the analysis lances to investigate the decarburization process at DEW were installed to measure the off-gas composition after the complete post-combustion, as schematically shown in **Figure 2**.
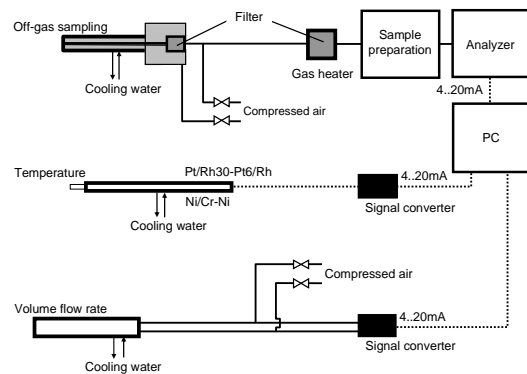


**Figure 3.** Sketch of off-gas analysing equipment (off-gas removal and analysing, temperature measurement, volume flow measurement and data acquisition)

The off-gas analysing system consists of water-cooled lances, filters, sensors, and signal converters to measure the composition of off-gas components. The infrared absorption spectrometry measures the CO and $CO_2$ concentrations while the paramagnetism principle is used to measure the $O_2$ concentration. The measured data of the off-gas compositions from the sensors was continuously recorded in a PC (**Figure 3**).

**Result of off-gas analysis.** The CO concentrations in off-gas at the chosen measurement point were found to be lower than 2000 ppm so that the contribution of CO concentrations to the total carbon mass balance were only up to 0.19 kg/t. For this reason, the installation of a CO sensor at this measurement point is less important when the off-gas analysing system is applied to monitor the decarburization process. This preliminary investigation demonstrated that the decarburization control by using the off-gas analysing system is applicable for both austenitic (**Figure 4**) and ferritic (**Figure 5**) stainless steel heats. The result of the off-gas analysis shows a higher second critical point for the ferritic heat compared to that of the austenitic heat. This is due to the higher carbon contents of ferritic stainless steel heats from a higher input of carbon-rich chromium alloy.
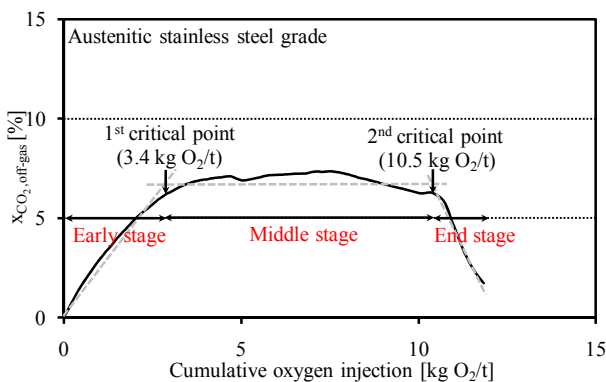


**Figure 4.** $CO_2$ concentration in off-gas during the refining period (an exemplary austenitic stainless steel heat)
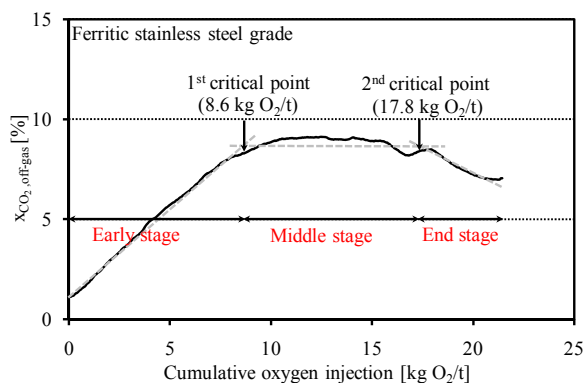


**Figure 5.** $CO_2$ concentration in off-gas during the refining period (an exemplary ferritic stainless steel heat)

Similar to the result of thermodynamic simulation, the result of off-gas analysis also demonstrated the existence of three consecutive decarburization stages, which is in agreement with the result of off-gas analysis at the BOF [7]. Nevertheless, some differences between the simulation result and the result of the off-gas analysis are clearly identified. The differences between the results of the off-gas analysis and the thermodynamic simulation exist as the elements oxidation does not merely depend on the thermodynamic phenomenon, but also on the other phenomena, e.g. mass and heat transfer, fluid mechanics, and kinetics. The differences are also due to the inhomogen temperature and elements distributions, mainly the oxygen distribution, inside liquid steel during the refining period. For instance, the hot injection zone lying directly after the oxygen lance has the highest oxygen concentration and temperature [7]. This leads to carbon oxidation in the early stage due to the restricted oxygen capacity of silicon in this zone. Since the off-gas analysis shows the occurrence of carbon oxidation in the early stage, chromium oxidation is also expected to begin in the early stage and it continues until the end stage. In contrast, the thermodynamic simulation result shows a neglectable chromium oxidation in the early stage. For this reason, oxygen injection should not be started if insufficient liquid steel, from melting of scrap and alloy elements, is present. In case the oxygen injection is too early started, the high volume flow rate of oxygen injection may result in excess chromium oxidation due to restricted oxygen capacity of silicon and carbon.

Silicon mass transfer in liquid steel controls the rate of silicon oxidation during the early stage of oxygen injection [8]. Meanwhile, the chemical reaction between carbon and oxygen at the steel-gas interface becomes the rate determining mechanism of decarburization in this early stage as carbon and oxygen mass transfers are sufficiently high in this stage [8-10]. The peak value of the decarburization rate and its duration in the middle stage depend on the flow rate of oxygen injection. The intensive

decarburization in the middle stage takes place until the carbon concentration in liquid steel reaches its critical value, which depends on the oxygen mass flow rate [7], temperature, CO partial pressure [8] as well as steel and slag compositions [11]. In the end stage of oxygen injection, mass transfer of carbon in liquid steel controls the decarburization rate [7]. After oxygen injection reaches the second critical point, carbon oxidation decreases. This is due to the decreasing carbon activity and also due to the decreasing driving force of decarburization kinetic, $[C] - [C]_{eq}$ in wt%, with the decreasing carbon concentration in liquid steel. Injection of argon gas with bottom purging plugs would increase the mass transfer coefficient of decarburization and decrease the equilibrium carbon concentration. Both increase the decarburization rate in the end stage. Since the EAF of the presented study is not equipped with argon bottom stirring, the CO product of liquid steel at tapping is higher than the equilibrium value. The required low carbon values are attained at DEW by subsequent stirring and degassing in a vacuum oxygen decarburization, VOD, process.

**Slag analyses.** The result of slag analyses performed for this preliminary investigation shows that the $Cr_2O_3$ concentrations in slag vary between 5.47 and 11.40 wt% (mean value 8.07 wt%), as depicted in **Table 2**. Relatively low FeO concentrations in slag demonstrate that iron is not intensively oxidized in the EAF. A synchronized analysis between the results of slag analyses, off-gas analysis, analysis of tapped steel, and thermodynamic simulation lead to a conclusion that higher FeO and $Cr_2O_3$ concentrations in slag are strongly correlated with higher excess oxygen in the end stage [11].

**Table 2.** Result of slag analyses (without the decarburization control)

|  | $Al_2O_3$ | CaO | FeO | MnO | $SiO_2$ | $Cr_2O_3$ |
|---|---|---|---|---|---|---|
| Mean | 4.52 | 36.35 | 3.26 | 3.60 | 29.31 | 8.07 |
| Standard deviation | 0.74 | 1.74 | 2.32 | 0.79 | 2.86 | 1.80 |

The result of slag analyses shows increasing FeO concentrations in slag with higher $Cr_2O_3$ concentrations (**Figure 6**). A positive correlation between the $Cr_2O_3$ and FeO concentrations possibly exists due to the simultaneous intensive chromium and iron oxidation by oxygen as well as due to the simultaneous reduction of chromium and iron oxides by silicon. Nevertheless, higher $Cr_2O_3$ and FeO concentrations in slag results in lower CaO concentrations. With the exception of FeO and CaO, no significant correlation between $Cr_2O_3$ and other slag components can be found in this case.
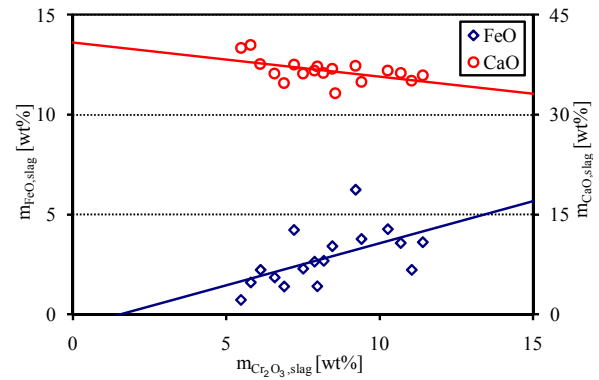


**Figure 6.** Correlations between the $Cr_2O_3$, FeO, and CaO concentrations in slag (without the decarburization control)
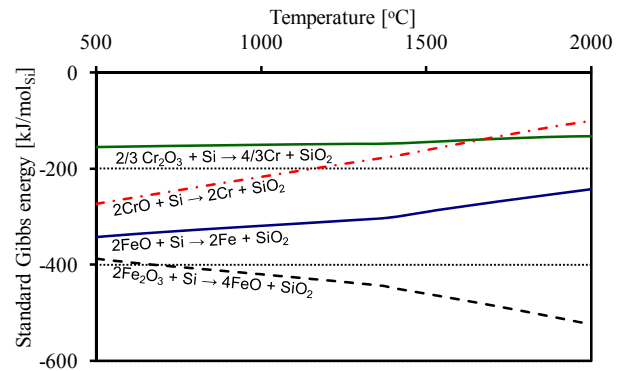


**Figure 7.** Standard Gibbs energy of $Fe_xO_y$ and $Cr_xO_y$ reduction by silicon

Silicon-based alloy is used as the sole reductant in the investigated EAF. $Cr_xO_y$ reduction by silicon thermodynamically competes with $Fe_xO_y$ reduction, since $Fe_xO_y$ reduction is thermodynamically more favourable than $Cr_xO_y$

reduction. This is due to more negative standard Gibbs energy of $Fe_xO_y$ reduction by silicon than that of $Cr_xO_y$ reduction (**Figure 7**). Pretorius [12] also demonstrated a competitive reduction of chromium and iron oxides by silicon. Low $Fe_xO_y$ concentrations in slag due to the efficient oxygen injection therefore benefits $Cr_xO_y$ reduction by silicon. Low $Fe_xO_y$ concentrations in slag also minimises chromium oxidation by $Fe_xO_y$ at the liquid steel-slag interface.

**Plant Trial of the Decarburization Control**

The plant trials were performed in an AC-EAF of DEW. A duplex process-route for stainless steelmaking at DEW involves an EAF and a VOD (**Figure 8**). The EAF melts down scrap, ferro-alloys, and other raw materials to produce liquid steel. The amounts of oxygen injection are in the range of 6 to 30 kg $O_2$/t depending on stainless steel grades. After tapping from the EAF, the liquid steel is charged into the VOD in order to achieve a very low carbon concentration.
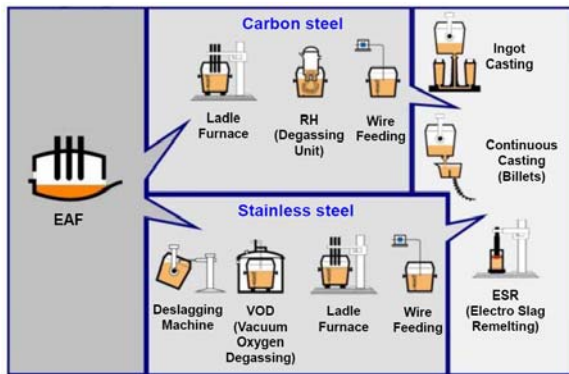
**Figure 8.** Routes and process units of carbon and stainless steels production at DEW

Water-cooled measurement lances used during the plant trials were specially designed by RWTH Aachen University. Meanwhile, an ABB continuous off-gas analysing system was used to analyse the off-gas composition. The off-gas composition was displayed on a com-

puter monitor located in the operator room so that the EAF operator can finish oxygen injection after the second critical point can be seen (**Figure 9**). In order to quantify the change of oxygen injection, the actual amount of oxygen injection was then compared with the set value, which had been pre-determined before the refining period started (eq. 1).

$$\Delta_{oxygen\ injection} = \frac{m_{O_2,actual} - m_{O_2,set}}{m_{O_2,set}} 100\ \% \quad (1)$$
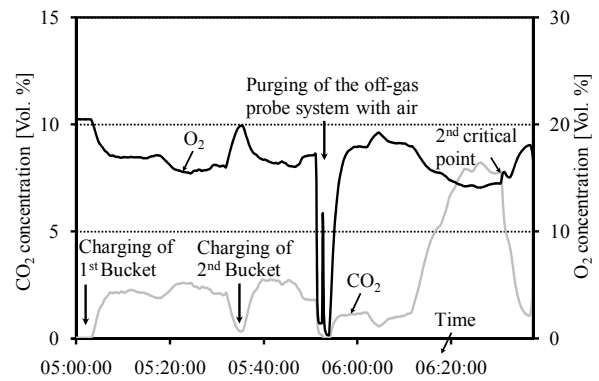
**Figure 9.** Off-gas composition of an exemplary stainless steel heat
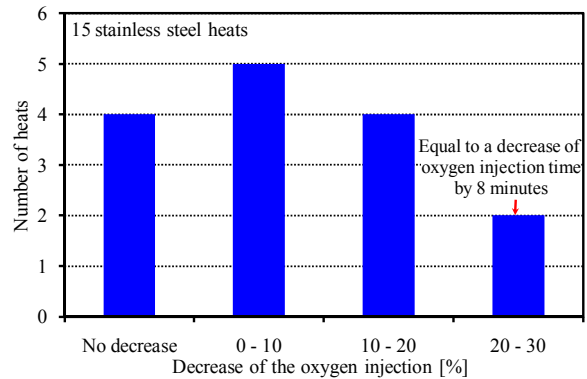
**Figure 10.** Decrease of the oxygen injection and its population during the plant trial phases 1 and 2

There were two phases of plant trial in this research. During the plant trial phase 1, oxygen injection was directly ended after the appearance of the second critical point and the amount of silicon was decreased below the pre-determined set value. The mass of silicon input during the plant trial phase 1 was intensely decreased as the amount of chromium and iron oxides in slag were ex-

pected to be lower. This strategy was performed to prevent excessively high silicon concentrations in tapped steel due to the non-reacted excess silicon. Silicon concentrations in tapped steel greater than the allowed level are forbidden. $SiO_2$, the oxidation product of silicon, is an aggressive substance for the ladle refractory during the VOD process so that a time-consuming second-deslagging process during the VOD process is a must. During the plant trial phase 2, oxygen was injected until the effective decarburization finished while silicon was charged in its nominal value.

The plant trial phases 1 and 2 delivered successful results. The decarburization control can prevent high carbon concentrations in tapped steel, i.e. higher than 1 wt%$_C$, since the second critical point was always in the range of 0.4 wt%$_C$ to 0.8 wt%$_C$. The oxygen consumption decreased for most heats. For a particular heat, the oxygen consumption could even be decreased by up to 24 %. This is equivalent to a decrease of oxygen injection time by up to 8 minutes (**Figure 10**). On the other hand, four heats showed that the amounts of oxygen injection were similar to or even higher than the initial set values. This circumstance may have indicated that the liquid steel had a higher carbon input than estimated from the available scrap database. For these four heats, the off-gas analysis showed no decrease of carbon concentrations in off-gas, i.e. the oxygen injection should have not been ended. However, oxygen injection could not be further continued for these particular heats, since it results in a very high temperature of the liquid steel. A very high temperature of liquid steel increases the wear rate of EAF refractory and causes a very high start temperature of the VOD process. This also increases the wear rate of ladle refractory.

**Table 3.** Result of slag analyses during the plant trial phase 2 (with the decarburization control)

| CID | $Al_2O_3$ | CaO | FeO | MnO | $SiO_2$ | $Cr_2O_3$ |
|---|---|---|---|---|---|---|
| Mean | 6.20 | 46.53 | 0.88 | 1.46 | 31.62 | 4.29 |
| Standard deviation | 1.83 | 3.02 | 0.36 | 0.55 | 2.97 | 2.14 |

As previously expected, the decrease of oxygen injecttion in the plant trial phase 1 did not result in high silicon concentrations in the tapped steel. Based on this positive result, silicon was charged in its nominal value during the plant trial phase 2 and oxygen injection was performed until the second critical point appeared, as performed during the plant trial phase 1.
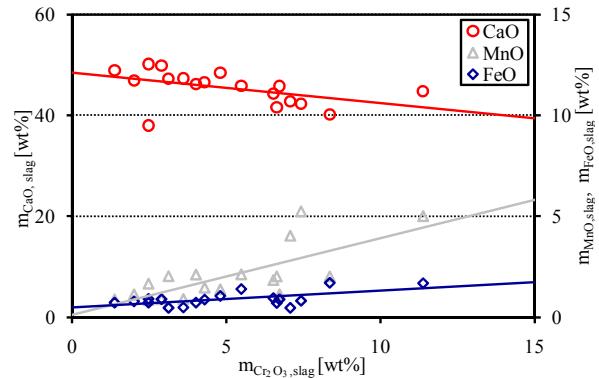


**Figure 11.** Correlations between the $Cr_2O_3$, MnO, FeO, and CaO concentrations in slag (plant trial phase 2)

**Table 4.** A comparison of the mean values of FeO and $Cr_2O_3$ mass in slag before and after the decarburization control by using the off-gas analysing system

| Case | FeO | $Cr_2O_3$ |
|---|---|---|
| | [kg/t] | |
| Without the decarburization control | 5.4 | 12.3 |
| With the decarburization control (plant trial phase 2) | 1.3 | 6.0 |

**The increase of chromium and iron yields.** As previously expected, the new strategy of oxygen injection was proven to significantly decrease chromium and iron oxidation (**Table 3**). The FeO concentrations vary between 0.47 wt% and 1.71 wt% (mean value 0.88 wt%) while the $Cr_2O_3$ concentrations are in the range of 1.37 wt% to 8.35 wt% (mean value 4.29 wt%). These mean values correspond to the decrease of FeO mass in slag by 76 % from 5.4 kg/t down to 1.30 kg/t. Meanwhile, the mean value of $Cr_2O_3$ mass in slag decreased by 51 % from 12.3 kg/t to 6.0 kg/t (**Table 4**), which is equivalent to a saving of chromium-alloy input by approximately 948 kg per heat. Lower $Fe_xO_y$ concentrations in slag can

decrease the wear rate of EAF refractory [7,8]. Less slag mass as well as less CaO input can be achieved due to lower $Cr_xO_y$ and $Fe_xO_y$ concentrations in slag. This leads to an additional economic benefit as less slag needs to be treated and deposited.

**Table 5.** Standard Gibbs energies of elements oxidation at 1873 K

| Reaction | dG [kJ/mol$_{O2}$] |
|---|---|
| $Si + O_2 \rightarrow SiO_2$ | -576 |
| $2Mn + O_2 \rightarrow 2MnO$ | -485 |
| $4/3Cr + O_2 \rightarrow 2/3Cr_2O_3$ | -435 |
| $2Fe + O_2 \rightarrow 2FeO$ | -296 |

Similar to the result of the slag analyses before the decarburization control, the result of the slag analyses after the decarburization control by using the off-gas analysing system also demonstrated the correlation between the $Cr_2O_3$, FeO, and CaO concentrations in slag (**Figure 11**). Moreover, it also showed a positive correlation between the $Cr_2O_3$ and MnO concentrations in slag. Based on this correlation, the intensive manganese oxidation is estimated to take place before the second critical point appears. The Ellingham Diagram shows that the standard Gibbs energy of manganese oxidation by oxygen is between the standard Gibbs energies of silicon and chromium oxidation (**Table 5**).

**Summary**

This research successfully develops the off-gas analysing system as a good control system of silicon, carbon, chromium, and iron oxidation during the refining period of stainless steelmaking in the EAF. The application of the off-gas analysing system to control the decarburization process in the EAF increases the efficiency of oxygen injection which leads to a decrease of oxygen injection for most heats. For a particular heat, oxygen injection could be decreased by up to 24 %, which is equivalent with the decrease of oxygen injection time by up to 8 minutes. For this reason, the EAF productivity can be increased.

During the plant trial, the decarburization control by using the off-gas analysing system decreased the mean values of chromium and iron oxides in slag by 76 % and 50 %, respectively. The decarburization control can also maintain the carbon concentration of tapped steel below 1 wt%$_C$. Since $Fe_xO_y$ concentrations in slag are low due to the efficient oxygen injection, a competitive $Fe_xO_y$ and $Cr_xO_y$ reduction by silicon can be avoided so that the consumption of silicon, as the sole reductant in the investigated EAF, can be well controlled. Less CaO input and less slag mass can be achieved due to lower $Cr_xO_y$ and $Fe_xO_y$ contents in slag. This leads to an additional economic benefit as less slag needs to be treated and deposited.

**Acknowledgement**

**References**

[1]  P. Sun, M. Uguccioni, M. Bryant, Ackroyd: Chromium control in the EAF during stainless steelmaking, Proc. of 55th Electric Furnace Conf., Chicago, USA, 9-12 November 1997, p. 297-302.

[2]  D. Senk, O. Wiens, L. Mavrommatis, L. F. Sancho, O. Rivas, N. Androutsopoulos, C. Galvao, J. J. Laserna, D. Papamantellos, C. Palangas, G. Angelopoulos: In situ, quick sensing system for measurements of critical components in steelmaking

slags, European Commission: Technical Steel Research, Luxembourg, 2007.

[3] K. Schwerdtfeger: Steel Research, 76 (2005), No. 8, p. 555-561.

[4] C. W. Bale, P. Chartrand, S. A. Degterov, J. Melançon, A.D. Pelton, G. Eriksson, K. Hack, S. Petersen: Calphad, 26 (2002), No. 2, p. 189-228.

[5] M. Kirschen, V. Velikorodov, H. Pfeifer, R. Kühn, S. Lenz, J. Loh, K. Schaefers: Proc. of 8th European Electric Steelmaking Conf., Birmingham, UK, 9-11 May 2005, p. 563-576

[6] M. Kirschen, H. Pfeifer, X. Tang: CFD Simulation der CO-Nachverbrennung für Lichtbogenöfen, 14. FOGI-Seminar, Essen, Germany, 04.-05.12.2002.

[7] B. Deo, R. Boom: Fundamentals of Steelmaking Metallurgy, Prentice Hall International, New York, USA, 1993.

[8] R. J. Fruehan: The Making, Shaping, and Treating of Steels: Steelmaking and Refining Volume, 11th Edition, Pittsburgh, USA, 1998.

[9] Y. G. Park, K. W. Yi: ISIJ International, 34 (1994), No. 9, p. 773-775.

[10] K. Taguchi, H. Ono Nakazato, T. Usui, K. Marukawa: Metallurgical and Materials Transactions B, 38B (2007), No. 1, p. 45-53.

[11] V. Y. Risonarta, L. Voj, H. P. Jung, S. Lenz, H. Pfeifer: Optimization of electric arc furnace process at Deutsche Edelstahlwerke, 9th European Electric Steelmaking Conf. Proc., 19-21 May 2008, Krakau, Poland.

[12] E. B. Pretorius, R. C. Nunnington: Stainless steel slag fundamentals-from furnace to tundish, Process Technology Conf. Proc., 2000, Orlando, USA, p. 1065-1087.